The Journal of the Astronautical Sciences, Vol. 52, No. 3, July–September 2004, pp. 000–000

An Improved Kalman Filter for Satellite Orbit Predictions

Paul Vergez[1], Luke Sauter[2], and Scott Dahlke[3]

Abstract

The nonlinear problem of tracking and predicting where a satellite will be over some time can be difficult with the recognition of modeling error and ground site radar tracking errors. For this reason it is important to have an accurate modeling program with the fidelity to correct for any errors in orbital motion and predict the most accurate positioning at some future time. The Extended Kalman Filter is one such program that can accurately determine position over time given estimate ranges for sources of error. However, the Extended Kalman Filter contains many linear approximations that allow its prediction and correction methods to work. This paper will discuss the effects of replacing the linearizing approaches made in the orbital model part of the program with numerical small-step approaches. The overall errors during prediction will be compared for an analysis of the corrective ability of the filter. Additionally a final prediction at a later date and another location will serve as an indicator to the usefulness of the prediction capabilities over time.

In exploring these effects, it will be shown that the linearizing approximations made in the development are a good approximation to the numerical results. The effects of modeling error, perturbation effects included, and the degree of approximation all play a significant role in accuracies of prediction. The effects of removing linearizations are small in comparison to the effects of perturbations and modeling error. The results of the numerical approximations contain a great robustness and as such help simplify the modeling process. The modeling process is discussed with reference to ADA program code. With these results it can be seen that there are several methods of using the Extended Kalman Filter for orbital prediction which maintain a high degree of accuracy and can be very useful when applied to real-world satellite prediction.

Introduction

The application of satellites takes many forms including international communications and television relay to space-based telescopes. However, a satellite's effectiveness is directly based on the ability to track and communicate with the spacecraft over its lifetime. In order to track a satellite, a ground station will use a site-defined coordinate frame to track the motion. This coordinate frame uses the

[1]Senior Associate Professor, Department of Aeronautics, United States Air Force Academy, CO 80840. Email: Paul.Vergez@usafa.af.mil.
[2]Associate Professor, Department of Astronautics, United States Air Force Academy, CO 80840. Email: Scott.Dahlke@usafa.af.mil.
[3]Second Lieutenant, United States Air Force Academy, CO 80840.

distance from the site to the satellite (ρ), the azimuth angle (Az), and the elevation angle (El) to determine where in the sky a satellite is at some time. The ability for a ground station site to find and track a satellite is based of the predictions made by mathematical models of the orbit. The more accurate a model can be at predicting a satellite's motion, the more successful a ground station will be at finding and tracking the satellite.

This paper discusses methods of improving an Extended Kalman Filter to improve the orbital determination and prediction process. Small perturbations felt by an orbiting body cannot be fully modeled. Additionally errors in the method of obtaining the actual position and velocity from radar data will cause errors. For these reasons it is essential to use a filtering device such as the Kalman Filter to statistically determine the most probable position of a satellite. This method also contains some errors in its prediction algorithms that take the form of mathematical linearizations. By seeking methods of reducing these linearizations this paper explores methods of improving the Extended Kalman Filter for better overall prediction and orbit determination. This approach has not been used before in the Extended Kalman Filter.

Because there are only a limited number of ground stations around the Earth, a satellite cannot be continuously tracked. Once a connection is lost, only the prediction of where the satellite will be at some later time can help in reestablishing communication. One of the most accurate methods of establishing a model that takes the orbital determination errors into account is the Extended Kalman Filter. The Extended Kalman Filter (EKF) is a stochastic estimation algorithm. The EKF simply uses a weighted statistical average of the difference in position and velocity inputs predicted from the model and known from the ground site to correct the model towards more precise predictions based on the known errors in those inputs. The EKF can be tuned to use anything from the basic two-body orbit model to highly accurate multi-perturbation model for its predictions. The effects of recognizing initial modeling error can also be explored making the EKF a valuable orbit prediction and modeling tool. Figure 1 shows the big picture of how the EKF is used in orbital modeling. Observations from one site allow for continual orbital model refinement and prediction to another site.

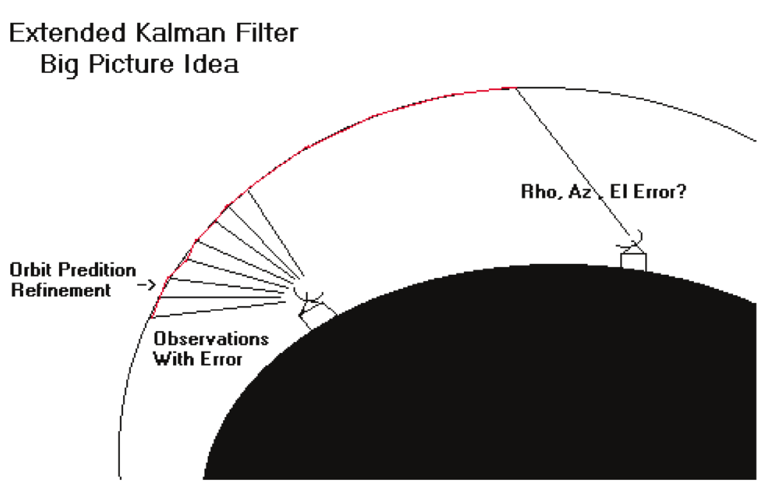

FIG. 1. Big Picture Model of Orbital Determination.

The normal Kalman Filter was created for linear applications. Because many systems like orbital motion are nonlinear, the extended filter makes many approximations to reduce nonlinear systems to linear models. For these reasons, the EKF has been the subject of several academic studies. At the Air Force Academy, an EKF was designed for an orbital determination scenario and the filter's stability was explored over a wide range of initial inputs and models [1]. The same initial EKF orbit model and scenario is explored in this paper. While the Academy's effort focused on the stability of the EKF on the initial orbit model, this paper expands from this to explore possible methods of optimizing the EKF results by removing linearizing assumptions made during the initial nonlinear reduction to a linear system.

By examining two methods of removing linearizations, this paper explores the effects of linear modeling assumptions as well as what inputs have the greatest effects on the orbit prediction. Linearizing approximations made during the creation of the EKF algorithm are replaced with numerical approximations that allow for nonlinear perturbation effects. The EKF algorithm attempts to minimize the difference in predicted and observed values at each ground site observation. To explore the effectiveness of removing linearization in the algorithm, the root mean square error in each site observation in position (**R**) and velocity (**V**) is explored over a pass of the Mahe Island ground station. Fifteen observations every twenty seconds are made during that pass. However, the true prediction power of the EKF comes from not only accurately predicting the next observation at the same ground station, but also accurately predicting an observation at another station over some large time. The errors in predicted ρ, Az, and El at the Thule ground station are also explored to determine the effects of removing linearizations. The idea of model refinement towards better predictions of the true orbit is similar to the theoretical mathematical model shown later in Fig. 2. The effects of initial model errors and the addition of perturbations to the model are also explored to determine the effectiveness of removing linearizations. With a better understanding of the issues involved in orbital determination and possible ways to improve these results, conclusions can be developed on the linearizing nature of the Extended Kalman Filter. The conclusions developed in this paper will allow more effective modeling of satellite motion for the insured use of these assets.

The Extended Kalman Filter

Initial Model Assumptions

The Extended Kalman Filter can be a very accurate model for orbital prediction; however, there are several assumptions that go into the design of the filter. The algorithm itself uses a basic model for satellite motion based on the two-body equation of motion. Several perturbation effects are added to this model in this paper, even though there is no way to fully capture all of the characteristics of a satellite's motion. The very nature of the statistical averaging in the algorithm also makes the assumption that none of the input data into the system are completely accurate once any error is specified in the input. As the filter attempts to further linearize the motion of a satellite over time, a first or second order Taylor series is used [2]. This approximation makes the assumption that only one or two terms of a Taylor series are a good approximation. These assumptions help to linearize the nonlinear problem of orbital motion. The purpose of this paper is to remove some of the linearization modeling assumptions in the Extended Kalman Filter.

Generalized Math Technique

The Extended Kalman Filter algorithm is made of two primary pieces, a prediction component and a correction component. Both of these components help to create an active algorithm that will statistically compensate a model of an orbit to minimize the observed and predicted position values and velocity state values. The EKF requires several initial inputs in order to work properly. These inputs include: the latitude, longitude, and altitude of the ground site; the individual radar site biases; the initial error covariance matrix (matrix P_i); the error expected from the radar site data (vector $\mathbf{R}_{\mathrm{error}}$); the estimated system dynamic modeling error (matrix Q_i); and the number and type of perturbation effects to consider [3]. The following perturbations are explored: J_2, J_3, J_4, drag, Sun, and Moon (the satellite's ballistic coefficient (BC) will be given to calculate the drag perturbation). In this project, either all or none of the possible perturbation effects are considered. The initial P_i matrix, $\mathbf{R}_{\mathrm{error}}$ vector, radar biases, and ground site data are given for this problem and will remain constant. The initial Q_i is either zero or 1×10^{-7}. (This is the same modeling error estimation assumed from the original Lyapunov Stability analysis.) The nature of these inputs are further explored throughout this paper. The Q_i, $\mathbf{R}_{\mathrm{error}}$, and P_i quantities are shown below in equations (1)–(3). The six-by-six nature allows for the position and velocity in each inertial axis to be represented. Additionally, the initial two-body state model is shown in equations (4) and (5). With these inputs and the initial model established, the EKF is posed to begin its stochastic estimation process.

$$Q_i = \begin{bmatrix} R\hat{i} & 0 & 0 & 0 & 0 & 0 \\ 0 & R\hat{j} & 0 & 0 & 0 & 0 \\ 0 & 0 & R\hat{k} & 0 & 0 & 0 \\ 0 & 0 & 0 & V\hat{i} & 0 & 0 \\ 0 & 0 & 0 & 0 & V\hat{j} & 0 \\ 0 & 0 & 0 & 0 & 0 & V\hat{k} \end{bmatrix} \tag{1}$$

$$\mathbf{R}_{\mathrm{error}} = \begin{bmatrix} \sigma\hat{i} \\ \sigma\hat{j} \\ \sigma\hat{k} \end{bmatrix} \tag{2}$$

$$P_i = \begin{bmatrix} R\hat{i} & 0 & 0 & 0 & 0 & 0 \\ 0 & R\hat{j} & 0 & 0 & 0 & 0 \\ 0 & 0 & R\hat{k} & 0 & 0 & 0 \\ 0 & 0 & 0 & V\hat{i} & 0 & 0 \\ 0 & 0 & 0 & 0 & V\hat{j} & 0 \\ 0 & 0 & 0 & 0 & 0 & V\hat{k} \end{bmatrix} \tag{3}$$

$$\mathbf{X} = \dot{\mathbf{R}} \tag{4}$$

$$\dot{\mathbf{X}} = \dot{\mathbf{V}} = -\frac{\mu}{R^2}\bar{\mathbf{R}} + \bar{\mathbf{A}}_{\mathrm{p}} \tag{5}$$

Prediction Process

The Extended Kalman Filter's primary purpose is to establish very accurate predictions of an orbit over time knowing the error that is expected in the model and the actual measurements [1, 2]. The satellite's motion is initially linearized to either a first or second order Taylor series transition matrix. This state transition matrix allows for the prediction of the states of position (**R**) and velocity (**V**) at some future time (Δt). The state transition matrix is based on the rate of change in **V** verses the rate of change of the **R** and is defined as the F matrix. Both the state transition matrix (ϕ) and the F matrix are shown in equations (6) and (7) respectively [2].

$$\phi = e^{-F(t)} = I + F\Delta t + F^2 \frac{\Delta t^2}{2!} \tag{6}$$

$$F = \frac{\partial \hat{\mathbf{X}}}{\partial \hat{\mathbf{X}}} \tag{7}$$

The Cowell method of orbit propagation is used to update the states and the error covariance matrix (P). The Cowell method of orbit determination uses the fourth order Runge-Kutta (RK4) approximation method to solve the differential equation for the new states (**X**) at some time (t_n). This differential equation can be seen below in equation (8), where variables with bars over the top are the predicted values and variables with hats are the corrected estimations. The RK4 method propagates the states over 100 time steps between every 20-second observation gap and between the long gap in time to the Thule site. Error covariance of the new states will be predicted from the state transition and the estimated error covariance as shown in equation (9). This idea can be seen in Fig. 2 showing the mathematical process of predicting and correcting the states end error over time [2].

$$\bar{\mathbf{X}}(t_n) = \int_{t_{n-1}}^{t_n} \dot{\hat{\mathbf{X}}}\, \mathrm{d}t + \hat{\mathbf{X}}(t_{n-1}) \tag{8}$$

$$\bar{P}(t_n) = \phi(t_n, t_{n-1})\hat{P}(t_{n-1})\phi^{\mathrm{T}}(t_n, t_{n-1}) \tag{9}$$

From estimated values, new predicted orbital values can be found, but these values are of little use for further propagation if they do not match the actual observations. This is where the correction process of the EKF identifies its usefulness. The first step in correcting the system is to establish the error between predicted values and actual observations. This is done through the H matrix as shown below in equation (10) [2]. Because it is known that the radar site data contains errors as well

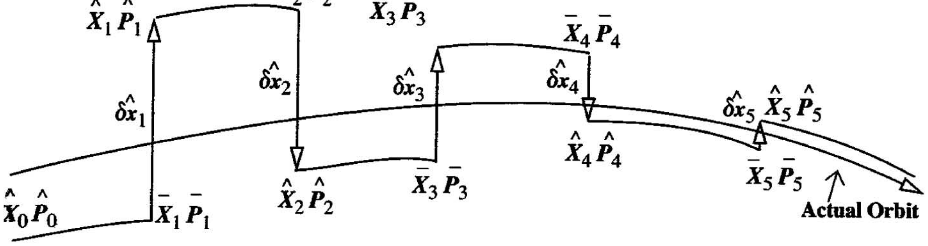

FIG. 2. Correction Process.

as the predictions, a statistical analysis process will be needed to correct the predictions and create new estimations of the states [4]. The next step in the process is the development of the Kalman Gain matrix (K). The K matrix uses the statistical weighed average of the predicted error covariance and the known radar site errors to establish a gain that will seek to minimize the diagonals of the estimated error covariance matrix. The K matrix can be seen in equation (11) [2]. With this data, estimations of the states and the error covariance can be created from a correction of the original predictions and the actual site information. These correction equations can be seen below in equations (12) and (13), where the $[\mathbf{Z} - g\mathbf{X}]$ term is the difference in the observed states versus the predicted states [2].

$$H(\bar{\mathbf{X}}(t_n)) = \frac{\partial g(\bar{\mathbf{X}}(t_n))}{\partial \bar{\mathbf{X}}(t_n)} \approx \frac{\Delta Observations}{\Delta \bar{\mathbf{X}}} \tag{10}$$

$$K(t_n) = P(t_n)H^{\mathrm{T}}[H\,P(t_n)\,H^{\mathrm{T}} + \mathbf{R}_{\mathrm{error}}]^{-1} \tag{11}$$

$$\hat{\mathbf{X}}(t_n) = \bar{\mathbf{X}}(t_n) + K[\mathbf{Z} - g\bar{\mathbf{X}}(t_n)] \tag{12}$$

$$\hat{P}(t_n) = [I - K\,H]\bar{P}(t_n) \tag{13}$$

Orbit and Measurement Performance

Orbit

The EKF scenario that is explored in this project is that of a satellite with the following set of orbital elements:

Semimajor Axis:	6697.0 km
Eccentricity:	0.0177
Inclination:	96.74°
Long. of the Ascending Node:	94.68°
Argument of Perigee:	57.35°
Mean Anomaly:	0.0°

The given satellite is the same as that used in the original Academy study [1]. This satellite is in a nearly circular low Earth orbit. A visual representation of this satellite and the monitoring ground stations can be seen in Fig. 3.

Measuring Sites and Performance Data

In order for an Extended Kalman Filter to work as an orbital optimization tool, it is necessary to have ground site observations of that orbit which can be used to correct the orbital model. Both the Mahe and Thule ground stations are used for this project and analysis. The Mahe ground station is located at 4.8° south and 55.5° east. This station will provide the primary measurements of the ρ, Az, and El of the satellite. These measurements can be easily converted to **R** and **V** vectors for the satellite given a known location and time of the observations. The date of these observations is 11 May 1995. The biases in the ground site radar and the noise expected from these observations can be seen in Table 1. Computer generated observations of the orbit with error can be seen in Table 2. The RMS error of these observations to the predicted results at each observation is used as one measure of performance. The orbital prediction capability of the EKF can then be compared to another ground site to determine the accuracy of the model. The second site used for observation is that of Thule, Greenland at 76.57° north and 68.3° west. The

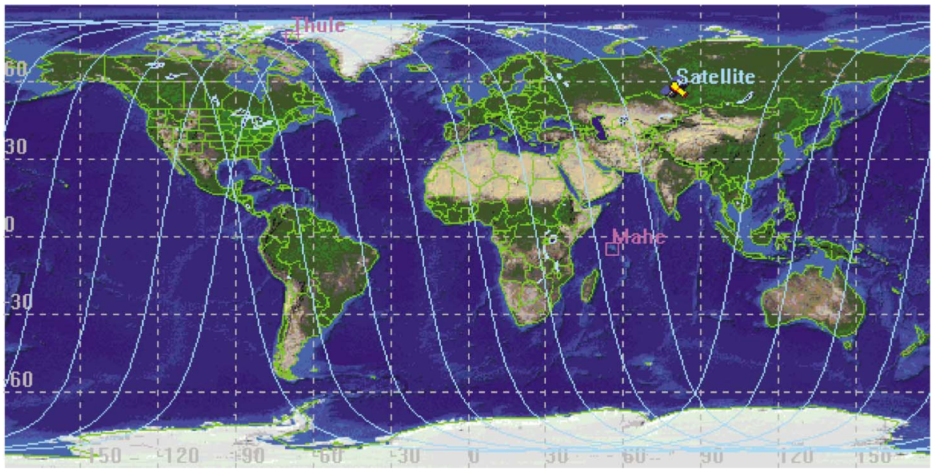

FIG. 3. STK Graphical Representation of Modeling Scenario.

biases and expected noise of this site can be seen in Table 3. This observation is made 21 minutes and 20 seconds after the last Mahe observation. Error difference between this observation and model's predicted results will be compared to provide another measure of performance [4, 5].

TABLE 1. Measurement Characteristics of Mahe Ground Station

Measurement	Biases	Standard Deviation σ
ρ (km)	0.15	0.15
Az (deg)	0.0001	0.01
El (deg)	0.0001	0.01

TABLE 2. Measurement Data from Mahe Ground Station

Hour	Minutes	Seconds	r (km)	Az (deg)	El (deg)
11	50	0	1770.334	195.1388	1.737
11	50	20	1636.96	197.6087	3.0125
11	50	40	1507.572	200.5082	4.414
11	51	0	1382.047	203.9435	5.8441
11	51	20	1262.499	208.0942	7.4128
11	51	40	1150.56	213.1119	9.0443
11	52	0	1049.464	219.2097	10.7308
11	52	20	961.3957	226.5796	12.3925
11	52	40	891.6892	235.4314	13.8777
11	53	0	844.4838	245.5759	14.9465
11	53	20	823.1501	256.6734	15.3395
11	53	40	829.9796	267.9568	14.9301
11	54	0	865.0305	278.6099	13.8245
11	54	20	924.6791	288.0676	12.2013
11	54	40	1003.953	296.0857	10.3958

TABLE 3. Measurement Characteristics of Thule Ground Station

Measurement	Biases	Standard Deviation σ
ρ (km)	0.0708	0.026
Az (deg)	0.0013	0.026
El (deg)	0.0075	0.022

Matching Results

In the analysis of an EKF, it is important to establish an accurate reference model from which to expand. First, the results of the initial Academy study were duplicated using the EKF in [1]. Several more accurate constants of motion and perturbation effects were added to this model. The results of the Academy's study were reproduced and a comparison of these results can be seen in Table 4. Matching these results helped establish a baseline for improvement.

Nominal Results

The following figures represent the possible input options and the error results for the Mahe observations. Some of the possible input options on the initial EKF are as follows: 1st versus 2nd order Taylor series, zero versus all perturbation effects, and zero versus 1×10^{-7} modeling error for the filter. It can be seen from these results that the largest difference in model results can be seen with the addition of modeling error. Both Figs. 4 and 5 show these results for the RMS position and velocity results respectively. It is important to note that all of the RMS error plots in this report are graphed with respect to the Julian date (JD) of observations. However, these observations are made twenty seconds apart as seen in Table 2.

Design Improvement Methods

The focus of this project is on the improvement of the EKF orbital determination modeling process. In particular, improving the EKF by removing linearizing assumptions will be explored. Assumptions on F and ϕ in particular are the interest of this analysis. These matrices are concerned with the prediction portion of the EKF [6, 7]. Improving the prediction process is one method of improving the overall modeling capability. There are many other methods of improvement that can be explored, however the biggest advantage in modeling capability would be the addition of all the known perturbation effects and the removal of these linearization results. For each of the linearizing assumptions, the mathematical techniques used to remove the assumption and the results of these changes are discussed in following sections. Many of the outlining causes of these results will be analyzed. Conclusions on possible uses of these results and nonlinearizations are discussed.

TABLE 4. EKF Data Matching Results Comparison: At Thule's First Observation Using Original 1995 Data

	Observed	Computed	Calculated Error	Error Results
Rho (km)	1194.8692	1205.322457	10.453257	**38.54**
Az (degs)	34.8631	35.53747	0.67437	**1.38**
El (degs)	**6.3154**	**6.569847**	**0.254447**	**0.78**

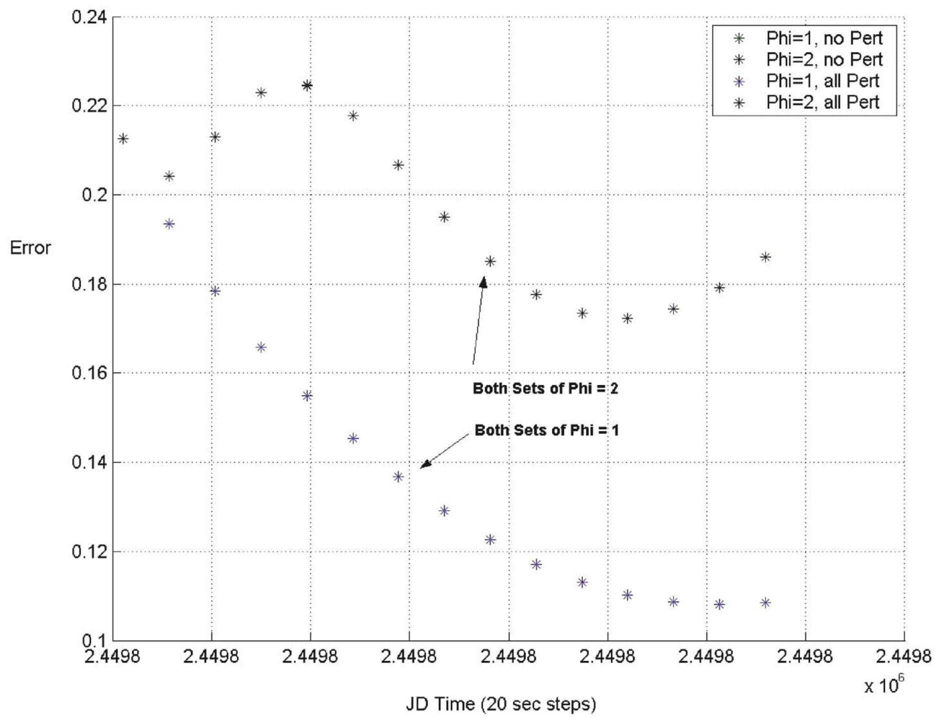

FIG. 4. Initial RMS Error Plot of Position (km) Including Modeling Error.

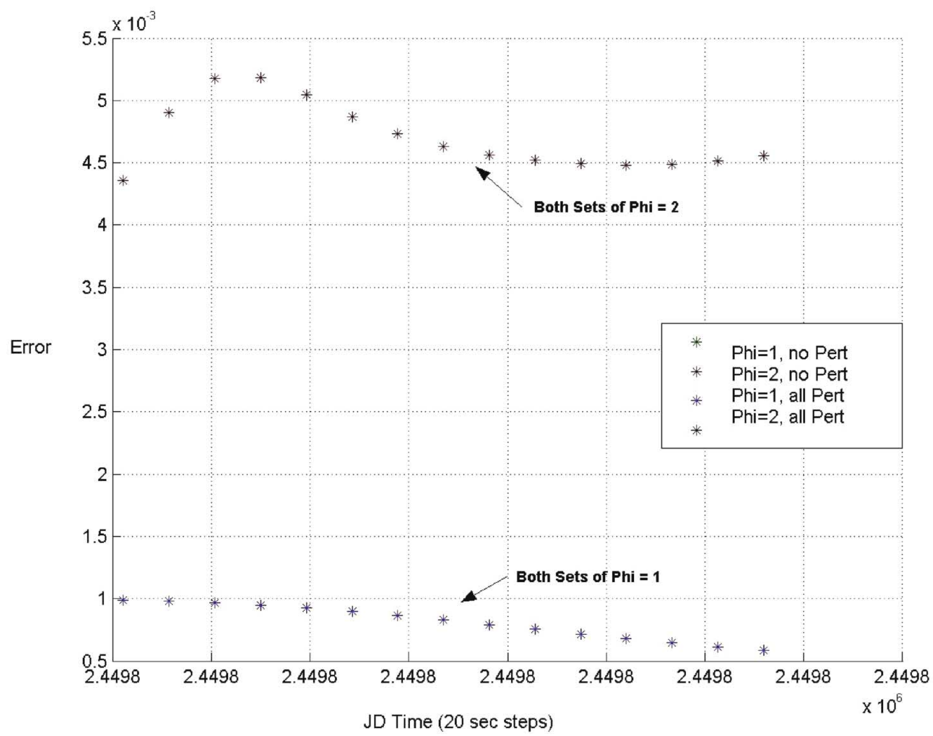

FIG. 5. Initial RMS Error Plot of Velocity (km/sec) Including Modeling Error.

F Matrix Nonlinearization

In the initial development of Extended Kalman Filter model, the change in the rates of change in the states versus the change in states themselves, or F matrix, is important to the understanding and modeling of orbital motion. The initial F matrix equation can be seen in equation (7). This equation is a very key component to developing orbital motion and the EKF algorithm. However, in order for the EKF to use this matrix, an analytic approximation approach must be used to reduce the equations of motion into a usable form. As seen in equation (14), most parts of the matrix go to zero or to identity except for one portion. Using only the two-body equations motion, analytic approximations for each of the terms in nontrivial portion of equation (14) can be found [2], [3], [5]. This lower nontrivial portion can be seen in equation (15). A series of nine equations can be painstakingly developed to solve for the final F matrix. However in the development of this approach to linearizing the F matrix differentials, many of the effective perturbation terms are lost and cannot be used in the orbital motion model [2].

$$F = \frac{\partial \dot{\hat{\mathbf{X}}}}{\partial \hat{\mathbf{X}}} = \begin{bmatrix} \frac{\partial \dot{\bar{\mathbf{R}}}}{\partial \bar{\mathbf{R}}} & \frac{\partial \dot{\bar{\mathbf{R}}}}{\partial \bar{\mathbf{V}}} \\ \frac{\partial \dot{\bar{\mathbf{V}}}}{\partial \bar{\mathbf{R}}} & \frac{\partial \dot{\bar{\mathbf{V}}}}{\partial \bar{\mathbf{V}}} \end{bmatrix} = \begin{bmatrix} 0 & I \\ \frac{\partial \dot{\bar{\mathbf{V}}}}{\partial \bar{\mathbf{R}}} & 0 \end{bmatrix} \tag{14}$$

$$\frac{\partial \dot{\bar{\mathbf{V}}}}{\partial \bar{\mathbf{R}}} = \begin{bmatrix} \frac{\partial A\hat{i}}{\partial R\hat{i}} & \frac{\partial A\hat{i}}{\partial R\hat{j}} & \frac{\partial A\hat{i}}{\partial R\hat{k}} \\ \frac{\partial A\hat{j}}{\partial R\hat{i}} & \frac{\partial A\hat{j}}{\partial R\hat{j}} & \frac{\partial A\hat{j}}{\partial R\hat{k}} \\ \frac{\partial A\hat{k}}{\partial R\hat{i}} & \frac{\partial A\hat{k}}{\partial R\hat{j}} & \frac{\partial A\hat{k}}{\partial R\hat{k}} \end{bmatrix} \tag{15}$$

The two-body acceleration is denoted by the components $A\hat{i}$, $A\hat{j}$, and $A\hat{k}$.

Mathematical Technique and Implementation

In order to remove this linearization effect and include all of the perturbation terms in the model another approach to creating the F matrix must be developed. The equation for this development can be seen in equation (16) below. The actual implementation of this equation requires a change in the position vector that is then feeding the change back into the RK4 prediction algorithm to determine the accelerations that would have been felt by that change. Small changes in each inertial direction (i, j, and k) for each term will complete the lower portion of equation (15). By assuming only small perturbations in the model, the small numerical changes in the rate of change in states can be compared to the small numerical changes in the states themselves. This approximation is very similar to the finite differential analysis development of the H matrix.

$$F \approx \begin{bmatrix} 0 & I \\ \frac{\Delta \dot{\bar{\mathbf{V}}}}{\Delta \bar{\mathbf{R}}} & 0 \end{bmatrix} \rightarrow Where\ \frac{\Delta \dot{\bar{\mathbf{V}}}}{\Delta \bar{\mathbf{R}}} = \begin{bmatrix} \frac{\Delta A\hat{i}}{\Delta R\hat{i}} & \frac{\Delta A\hat{i}}{\Delta R\hat{j}} & \frac{\Delta A\hat{i}}{\Delta R\hat{k}} \\ \frac{\Delta A\hat{j}}{\Delta R\hat{i}} & \frac{\Delta A\hat{j}}{\Delta R\hat{j}} & \frac{\Delta A\hat{j}}{\Delta R\hat{k}} \\ \frac{\Delta A\hat{k}}{\Delta R\hat{i}} & \frac{\Delta A\hat{k}}{\Delta R\hat{j}} & \frac{\Delta A\hat{k}}{\Delta R\hat{k}} \end{bmatrix} \tag{16}$$

Note that the acceleration now includes two-body accelerations as well as all the requested perturbation accelerations.

In the development of this approach it is necessary to understand what sort of "small" step in position will accurately model the acceleration perturbations that may be felt. To get an idea of the needed step size in position that should be taken, the acceleration felt by the system was graphed with respect to the position. These results can be seen in Figs. 6 and 7. By inspection, a position step size of $0.001R$, roughly 6 km, should be able to accurately model the perturbations. This is because a small size is needed to model the curl at the end of the acceleration in the **j** direction. However, to ensure these results, the step size was tested over a wide range as seen in the comparison figures.

Results

The result of this implementation in the Extended Kalman Filter algorithm can be seen in the sets of data from both the Mahe and Thule ground stations. The RMS error in both **R** and **V** were plotted versus time of the observation. These results compared with this nominal model results and the same inputs can be seen in the figures. As can be seen from these results, there is relatively no difference in the modeling ability of the new numerical F approach. These results are displayed in Figs. 8 and 9. To explore what effects differing step sizes would have a range of multiplication factors were input into the same model as can be seen in Fig. 10. Due to the fact that the small position changes will only affect velocity terms, only the RMS velocity errors will be shown to explore different step sizes. These results can be seen in Fig. 10. Figure 11 goes on to explore the effects of modeling error on the numerical F matrix, again only the velocity is shown because that is the only

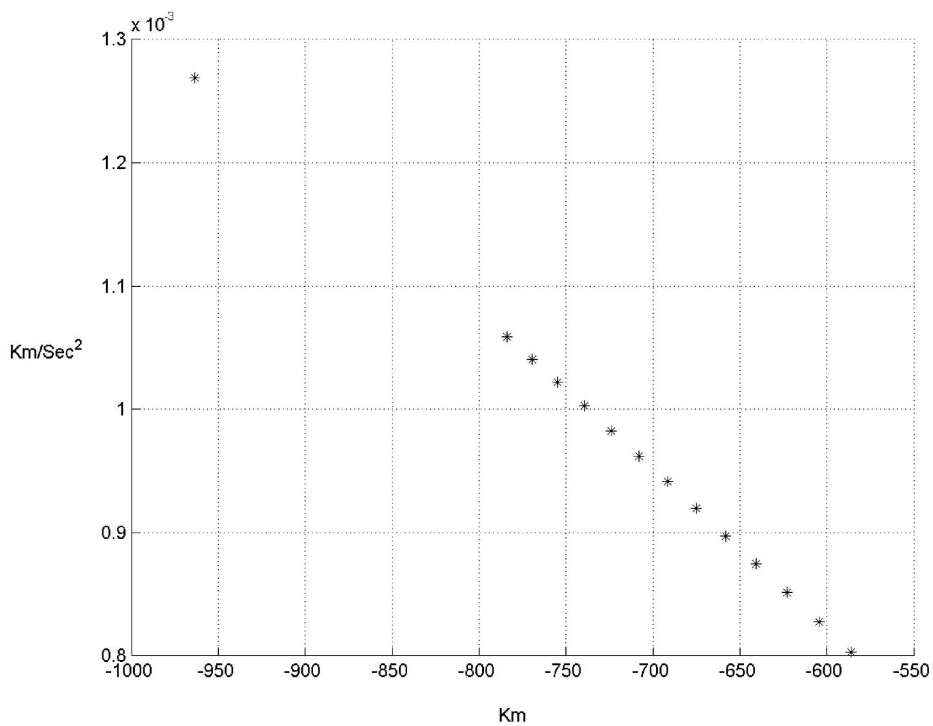

FIG. 6. Acceleration Versus Position Curve in the i and k Directions.

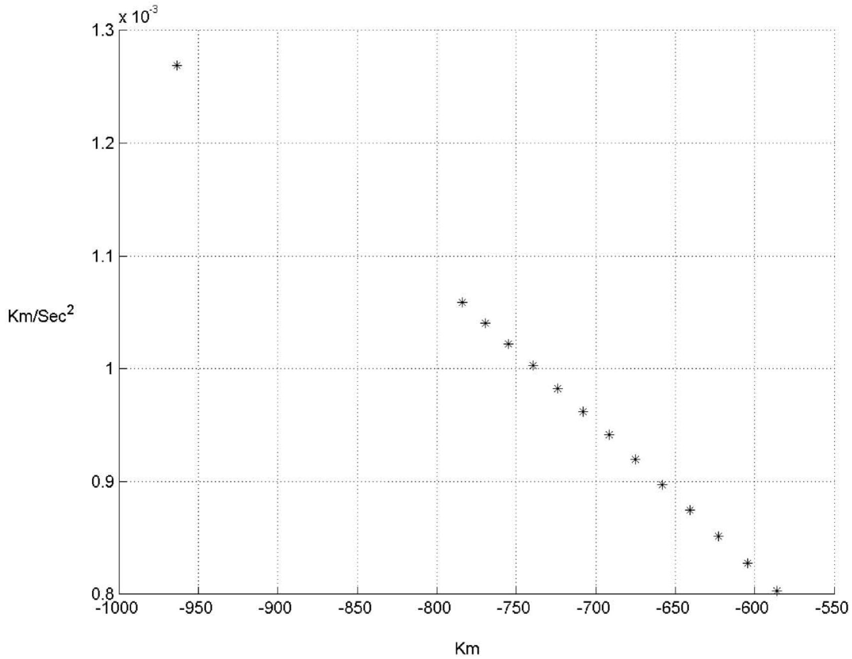

FIG. 7. Acceleration Versus Position Curve in the j Direction.

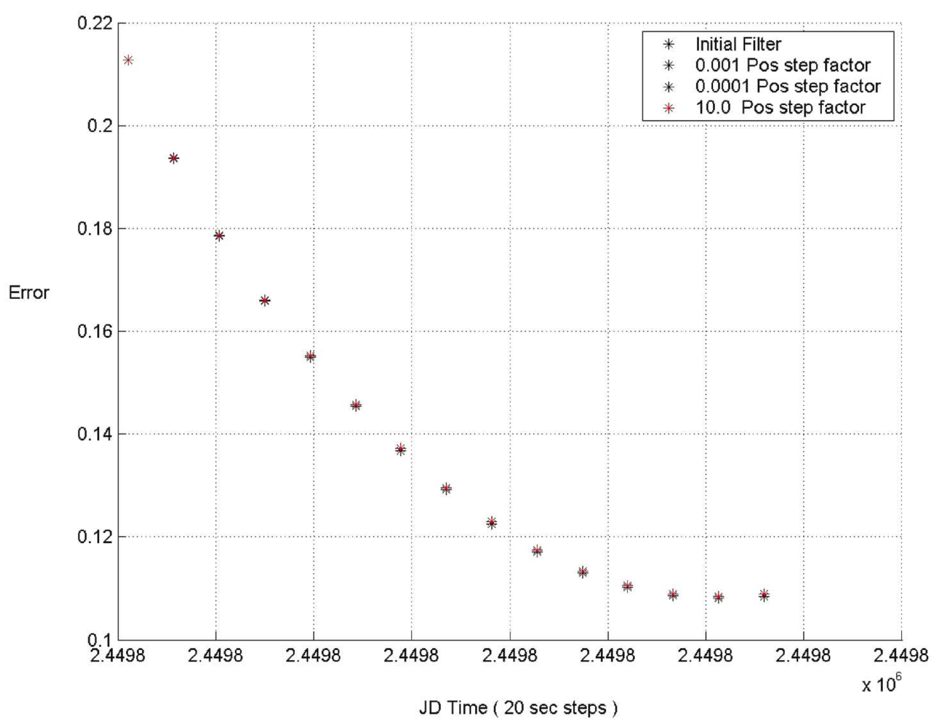

FIG. 8. Numerical F Matrix RMS Error Plot Comparison of Position (km).

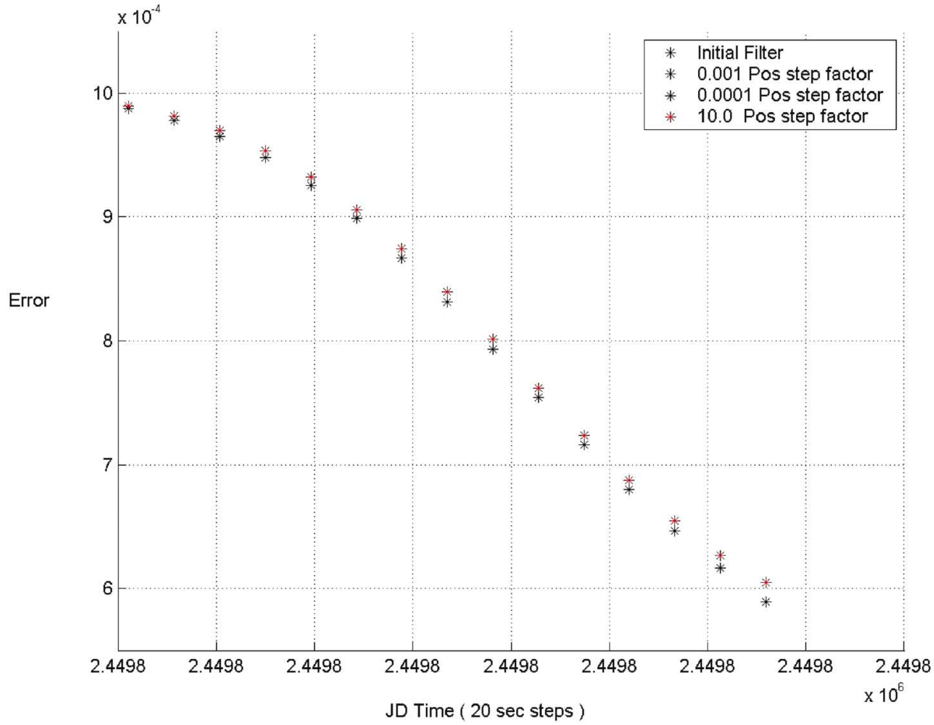

FIG. 9. Numerical F Matrix RMS Error Plot Comparison of Velocity (km/sec).

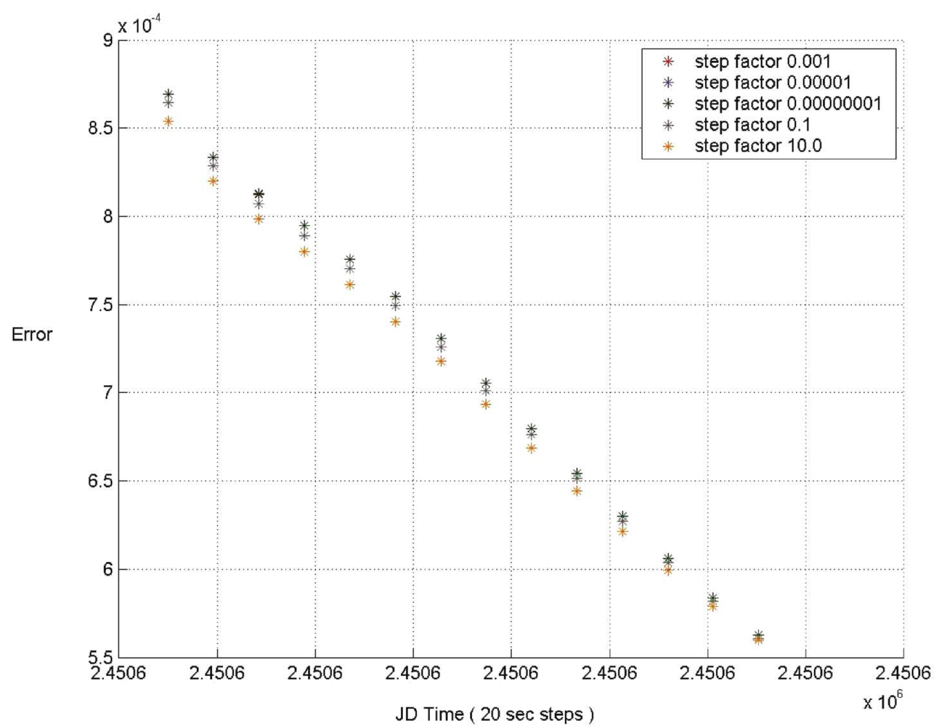

FIG. 10. Numerical F Matrix RMS Error Plot of Velocity with Position Step Factor Comparison.

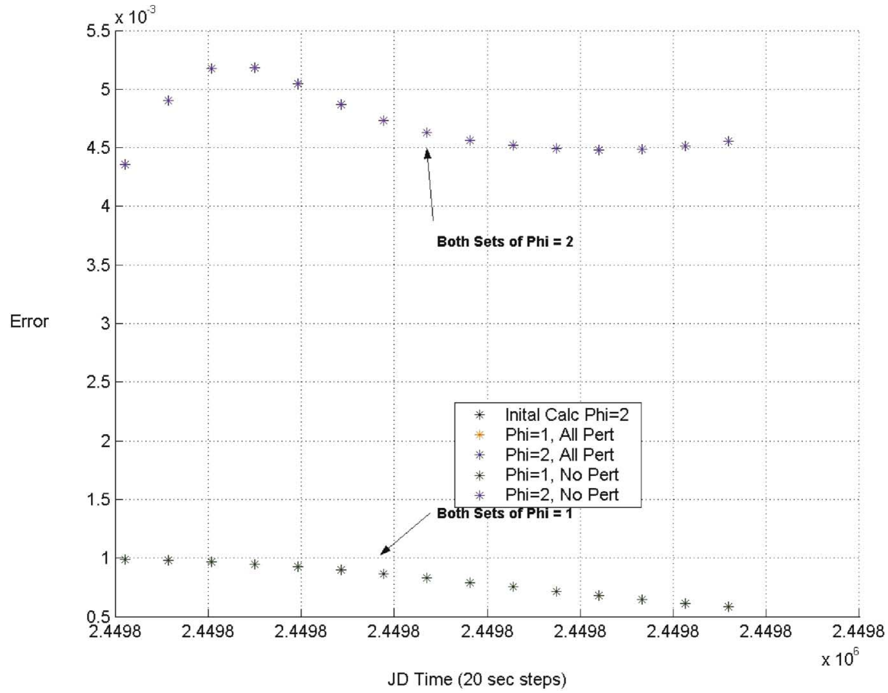

FIG. 11. Numerical *F* Matrix RMS Error Plot of Velocity with Modeling Error (Step Factor = 0.001).

factor that experiences any observable effect. It can also be seen from these graphs that using a second order Taylor series approximation will yield results similar to the initial results, which include modeling error. However, using only a first order Taylor series will negate the effects of any modeling error. The best results come from the largest step size multiplication factor, roughly 60 km. These results are very small and have virtually no effect on the system. For all purposes the step size is not that significant of a factor in the *F* matrix approximation.

To examine the effects of this *F* matrix correction, several inputs were varied and the RMS outputs were plotted. These results from varying the Taylor series approximation are used and the number of perturbation effects can be seen in the previous Figs. 10 and 11. The results appear to be very similar to those of the previous cases. However there are larger and more variable RMS error results with the second-order Taylor series. Upon inspection of all of the final Thule results of the test cases with their variable changes, an interesting fact arises. The cases where all of the perturbation effects were added to the model produce better results. However, the cases that include a second-order modeling term are far more accurate than all of the above. These error results in the predicted versus actual ρ, Az, and El can be seen in Table 5. This table includes all of the initial test cases with the original EKF as well as all of the test results with the new numerical *F* matrix approach. It is also important to note that there was no effect on these results with the implementation of modeling error when a first order Taylor series approximation was used.

Numerical F Matrix Conclusions

It can be seen from the results above that the largest variation in modeling results comes from the accuracy of the order of the ϕ matrix Taylor series approximation.

TABLE 5. **Thule Ground Site Error Results Comparison with New F Matrix**

Initial EKF

	1st order TS No Perturbations	1st order TS With Perturbations	2nd order TS No Perturbations	2nd order TS With Perturbations
Rho (km)	16.52199	10.440295	3.745989	−0.883965
Az (deg)	0.762506	0.674056	0.009566	−0.022303
El (deg)	0.475505	0.253603	0.27798	−0.003839

TS—Taylor Series

EKF with new F-matrix

	1st order TS No Perts. Factor = 0.001	1st order TS With Perts. Factor = 0.001	2nd order TS No Perts. Factor = 0.001	2nd order TS With Perts. Factor = 0.001	2nd order TS No Perts. Factor = 0.0001	2nd order TS With Perts. Factor = 0.0001
Rho (km)	16.522063	10.440655	3.745981	−0.88397	3.745989	−0.883958
Az (deg)	0.762527	0.674062	0.009566	−0.022303	0.009566	−0.022303
El (deg)	0.475491	0.253633	0.27798	−0.00384	0.27798	−0.00384

The use of the second order Taylor series is accurate enough to actually capture the effects of a modeling error. The results from each test case nearly match all of the initial data results with similar initial configurations. In cases where more error arose than the initial model, it appears that more rounding error played a part in looking at the small acceleration changes. The F matrix still relies on the RK4 algorithm, which inherently contains some error. In conclusion, it seems that the F matrix two-body linearization is a good assumption to make, and the largest differences come in the manipulation of the state transition matrix. The results using a better ϕ matrix approximation are significantly greater and thus beg for a better understanding. For this reason completely removing the Taylor series approximation and the need for the F matrix from the ϕ matrix is explored.

ϕ Matrix Nonlinearization

The ϕ matrix is the state transition matrix of the Extended Kalman Filter. This matrix allows the filter to predict how the error covariance of the states will change with time [2]. In the current use of the EKF, the ϕ matrix is approximated by a second order Taylor series as seen in equation (6). However, this approximation can cause error in the loss of the higher order Taylor series terms used to solve the differential equation shown in equation (17). This equation is from what derives the initial need for the F matrix. By using a different approach, the idea of a state transition matrix can be solved without the need of a differential equation, and thus without the need of the Taylor series or the F matrix.

$$\dot{\phi} = F\phi \tag{17}$$

Mathematical Technique and Implementation

The ϕ matrix is merely the equations of state necessary to transfer from the initial states to some final state [6]. This relationship can be seen in equation (18) [2]. Much like the numerical finite differential analysis approach taken with F, the ϕ matrix will perturb an initial state and propagate it forward to compare it with the nominal propagated state. By establishing the difference in perturbations results in each direction compared to the initial perturbations, the ϕ matrix can be directly solved for as seen in equation (19).

$$\delta\mathbf{X} = \phi\, \delta\mathbf{X} \tag{18}$$

$$\phi = \delta\mathbf{X}\,(\delta\mathbf{X}_{\text{initial}})^{-1} = \begin{bmatrix} \delta Xi & \delta Xj & \delta Xk & \delta Vi & \delta Vj & \delta Vk \\ \downarrow & \downarrow & \downarrow & \downarrow & \downarrow & \downarrow \\ & & \delta\,\text{Results} & & & \\ & & & & & \\ & & & & & \end{bmatrix} \begin{bmatrix} \delta Xi & 0 & 0 & 0 & 0 & 0 \\ 0 & \delta Xj & 0 & 0 & 0 & 0 \\ 0 & 0 & \delta Xk & 0 & 0 & 0 \\ 0 & 0 & 0 & \delta Vi & 0 & 0 \\ 0 & 0 & 0 & 0 & \delta Vj & 0 \\ 0 & 0 & 0 & 0 & 0 & \delta Vk \end{bmatrix}_{\text{initial}}^{-1} \tag{19}$$

Results

The results of this simple algorithm are very elegant and also very surprising. In the establishment of the new algorithm, it was once again necessary to determine a proper step size in position. The ratio of the position step size to the velocity step size is also a variable to be determined. The ratio value of 0.001 (which was used in previous studies) seemed the best choice since the velocity was on average three orders of magnitude less than the position. The effects of perturbations in the orbit as well as the effects of modeling error were explored in this analysis. The comparison of these variables with the initial estimate at position step size (dx) and ratio factors can be seen in Figs. 12 and 13. The greatest effects on the data in this case occur when the modeling error is applied. When compared to the results from the initial filter plots, these plots are nearly identical (this result can also be seen in the Thule data site comparisons). The use of modeling error matches the second-order Taylor series approximation and without the use of modeling error matches the first-order results. These initial results can be found in Figs. 4 and 5. In the comparison, when looking at the RMS error velocity plots of varying dx and ratio values over several orders of magnitude, it can be seen that there is hardly any change in prediction errors. These comparison graphs can be seen in Figs. 14 and 15 respectively. Once again only the velocity graphs are shown here because they show the actual correlation to the new changes in adding acceleration terms. These results show that the new numerical ϕ approach is very robust and eliminates the need for precise refinement when it comes to the dx and ratio estimations.

The final prediction data produced from all of the possible test cases at the Thule ground can be seen in Table 6. This data also includes a more robust set of varied

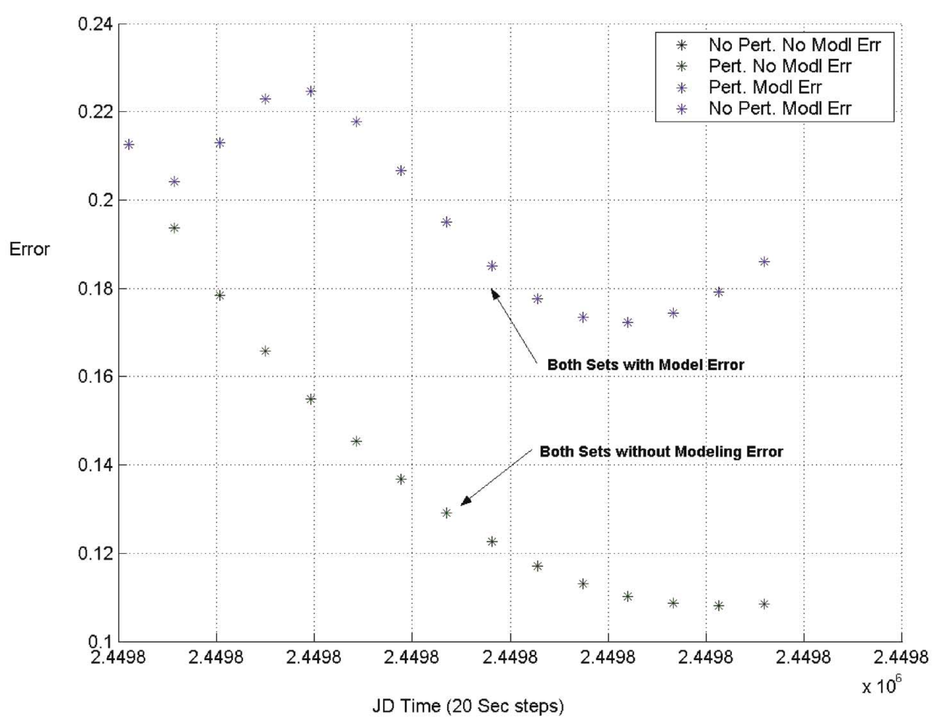

FIG. 12. Numerical ϕ Matrix RMS Error Plot Comparison of Position (km).

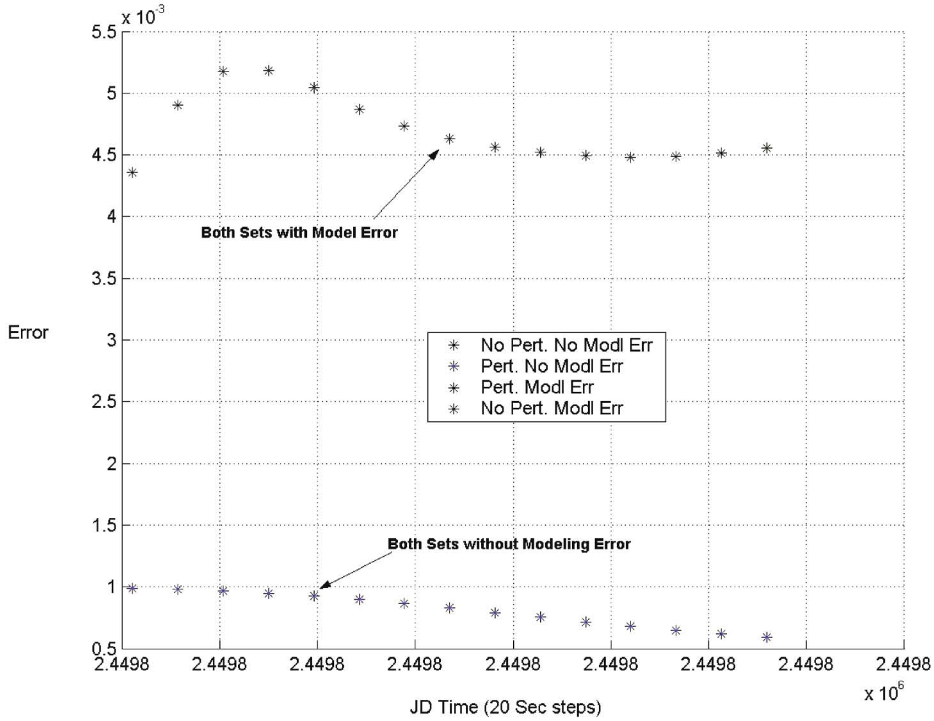

FIG. 13. Numerical ϕ Matrix RMS Error Plot Comparison of Velocity (km/sec).

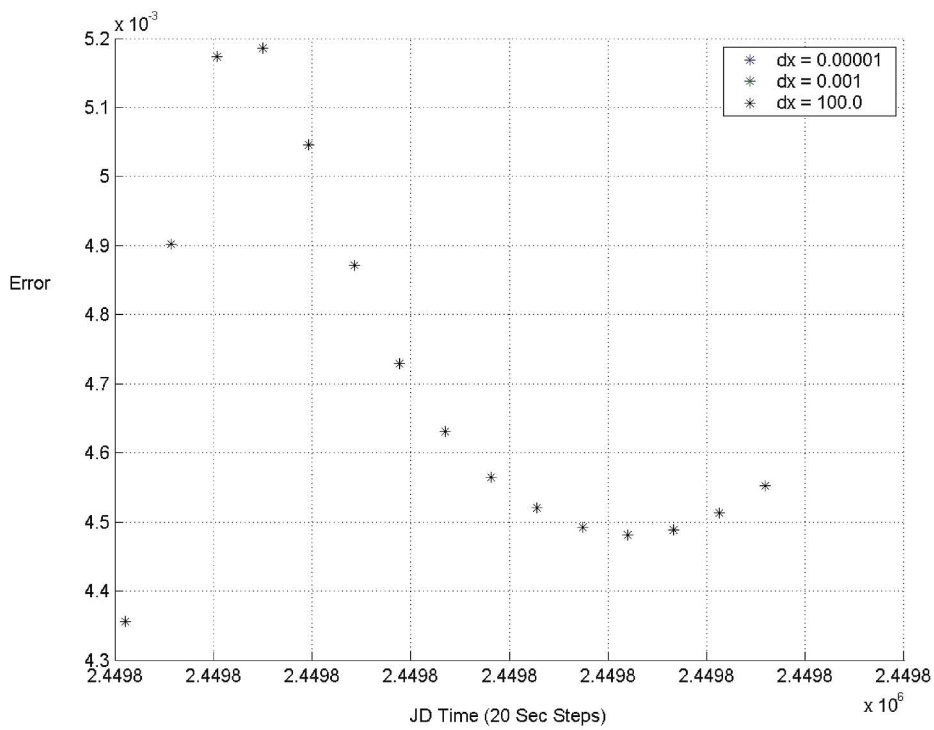

FIG. 14. Numerical ϕ Matrix RMS Error Plot of Velocity (km/sec) with dx Step Factor.

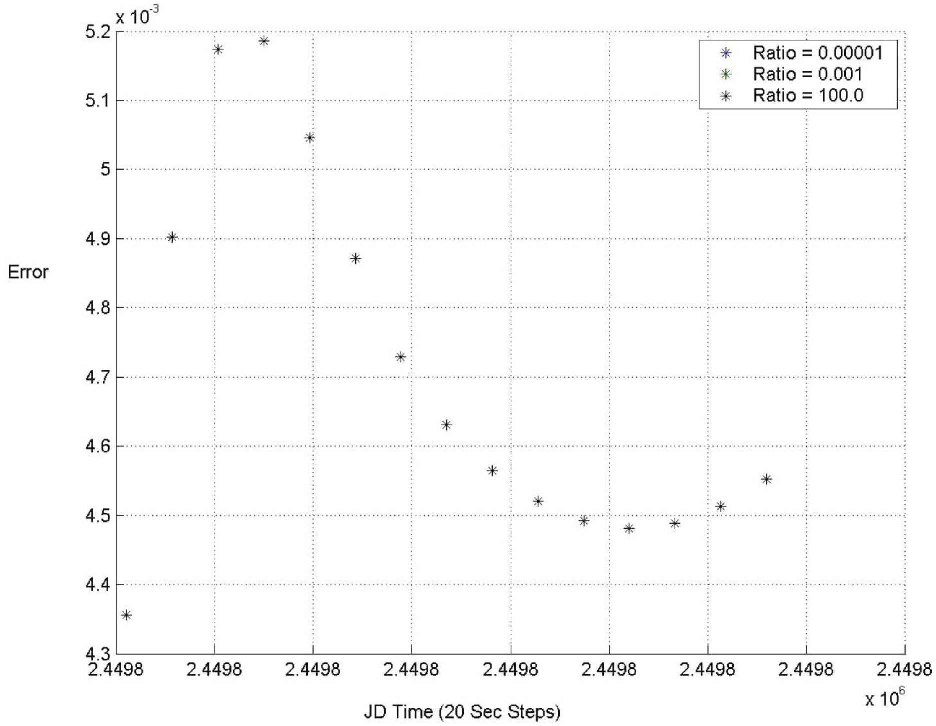

FIG. 15. Numerical ϕ Matrix RMS Error Plot of Velocity (km/sec) with Ratio Step Factor Comparison.

dx and ratio results and can be compared to the initial EKF results found in Table 5. In this table, it can be seen that the first four cases involving the perturbations and the modeling error nearly match the initial model results with the same variable changes. These results help to show that the method works in its approximation and that it is slightly more consistent than the original approximation. The unusual result from this entire test is in the fact that the model is very robust at handling a large range in position and velocities step sizes. The model was tested to breaking, failing the code, in the maximum (925 step factor) and minimum (1×10^{-7} step factor), in allowable ranges of *dx* and in ratio step size multiplication factors. These tests produced no significant improvement in results other than the proof that the model is very robust. In looking at the direct compensation error value, $[\mathbf{Z} - g\mathbf{X}]$, that goes into the Kalman gain matrix to correct the system after each prediction, the filter worked hard to correct the difference down to zero. Again there was no response to varying the *dx* value used. These results are shown in Fig. 16. The predicted mathematic modeling process from Fig. 2 is reminiscent of the actual process shown in Fig. 16.

Numerical ϕ Matrix Conclusions

It can be seen from these results that the approach of removing the linearizing approximations in the ϕ matrix and allowing for all of the perturbation effects allows the EKF to become very robust at modeling data of any sort. While it is still not completely understood how the EKF can handle such a wide range in step size inputs, it is plain to see that the best results come from the use of modeling error and including all of the possible perturbation effects. This approximation is very

TABLE 6. Thule Ground Site Error Results Comparison with New ϕ Matrix

dx = ratio =	0.001 0.001	0.00001 0.001	0.0001 0.001	0.01 0.001	1.0 0.001	100 0.001
Rho Error (km)	−0.883436	−0.883476	−0.883437	−0.883436	−0.883437	−0.883488
Az Error (deg)	−0.022292	−0.022294	−0.022292	−0.022292	−0.022292	−0.022292
El Error (deg)	−0.003827	−0.003828	−0.003827	−0.003827	−0.003827	−0.003825

dx = ratio =	0.00001 0.00001	1.0 1.0	0.001 0.00001	0.001 0.0001	0.001 0.01	0.001 1.0	0.001 100
Rho Error (km)	−0.883518	−0.883438	−0.883426	−0.883432	−0.883436	−0.883436	−0.883436
Az Error (deg)	−0.022295	−0.022292	−0.022292	−0.022292	−0.022292	−0.022292	−0.022292
El Error (deg)	−0.003824	−0.003827	−0.003827	−0.003827	−0.003827	−0.003827	−0.003827

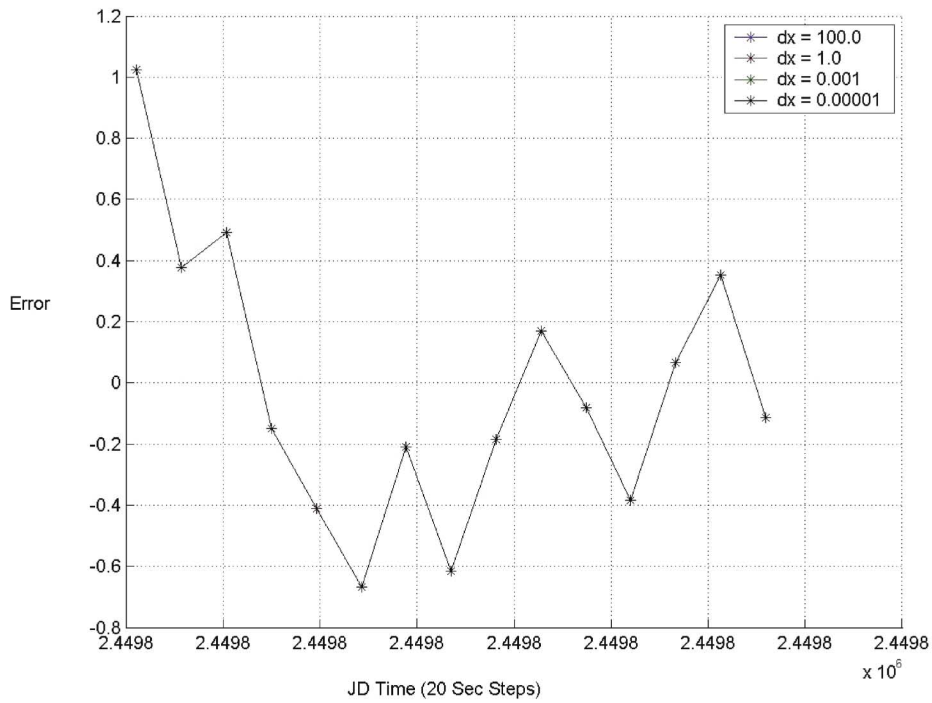

FIG. 16. Numerical f Matrix Direct Compensation Error Value, $[\mathbf{Z} - g\mathbf{X}]$.

easy to implement in code and serves as a great modeling source as it is consistently better than any other approximation method. This ϕ matrix fix should be implemented in future uses to improve the filter operations. This is because it is constantly accurate while allowing for a robust range of step inputs and the use of an imperfect model.

Overall Conclusions and Recommendations

It has always been the pursuit of science and engineering to try and find the best way to produce the most accurate results. In the case of the Extended Kalman Filter, it is very hard to create the better mousetrap of orbital determination and modeling. The Kalman filter is not just a simple process but involves a variety of external inputs, complex matrix operations, and statistical determination to create an optimizing algorithm for orbital determination. In the approach of removing linearizing assumptions made during the initial creation of the EKF, it can be seen that the results are not significantly better than those with the linear approximations. It appears that the greatest improvement in results comes from knowing how to set up the filter and what inputs are necessary. In looking at the comparison results of each method, it appears that the model inputs used have the largest effects on the system. These results also serve to prove the fact that the initial linearizations and approximations created are a fairly accurate representation of the actual process. In light of the results of the ϕ matrix improvement, it is recommended that this change be added in future systems. This matrix allows for a decrease in needed inputs into the model and allows for a wide range of possible step multiplication factors. This system would help ease implementation into orbital determination problems where the modeling accuracy is never truly zero. While the perfect orbital determination software can never be developed to handle all satellites, the Extended Kalman Filter does a remarkable job of orbital modeling given some initial observations for further optimization.

This approach to removing some of the linearization in the system model is not unique to the orbital determination problem. It is general enough that it can be applied to the estimation of almost any nonlinear system.

References

[1] VERGEZ, P. L. *Lyapunov Stability Analysis of an Orbit Determination Problem, The Journal of the Astronautical Sciences,* Vol. 45, No. 2, April–June 1997, pp. 233–245.

[2] VALLADO, D. A. *Fundamentals of Astrodynamics and Applications,* Space Technology Series, McGraw Hill, 1997.

[3] BATE, R. R, MUELLER, D. D, WHITE, J. E. *Fundamentals of Astrodynamics,* Dover Publications, Inc., New York, NY, 1971.

[4] RIGGS, JR., T. L. and VERGEZ, P. L. "Advanced Air-To-Air Missile Guidance Using Optimal Control And Estimation," AFATL-TR-81-56 Defense Technical Information Center, Eglin AFB, Florida, 1981.

[5] SELLERS, J. J. *Understanding Space: An Introduction to Astronautics.* McGraw-Hill, Inc., New York, NY, 1994.

[6] The Analytic Sciences Corporation "Applied Optimal Estimation," Gelb, Arthur, editor, 1974.

[7] WELSH, G. and BISHOP, G. "An Introduction to the Kalman Filter," TR 95-041, Department of Computer Science University of North Carolina at Chapel Hill, Chapel Hill, NC, 2001.